J Nanopart Res (2008) 10:39–57
DOI 10.1007/s11051-008-9427-7

REVIEW PAPER

Plasma synthesis of nanopowders

Dieter Vollath

Received: 10 January 2008 / Accepted: 21 May 2008 / Published online: 10 June 2008

Abstract There is a huge variety of plasma processes for synthesis of nanoparticulate powders. They may be grouped with respect to operating temperature, which is the essential parameter with respect to the properties of the products. In view of industrial production, the highest degree of maturity is found in high temperature processes working under ambient pressure. For products, where well-defined properties are demanded, low temperature microwave plasma processes are best suited. Additionally, these processes allow coating of the produced particles, even with organic phases. Other processes where plasmas are involved, such as laser or flame processes coupled with electric fields have, to some extent, a high potential for development.

Keywords Nanoparticles · Plasma processes · RF processes · Microwave synthesis · Laser synthesis · Coated particles · Nanotechnology · Nanomanufacturing

Introduction

This article is an attempt for a systematic description of plasma processes for the synthesis of nanopowders. Plasma processes are a special variety of gas phase processes with a bundle of essential advantages. Most important are the high efficiency with respect to energy consumption and—in case of proper selection of operating conditions—extreme narrow particle size distributions. Narrow particle size distributions are obtained, because particle formation in plasma synthesis is, in contrast to conventional gas phase synthesis, not necessarily a random process, rather, it may be controlled by particle charging. There are many different demands with respect to product quality and quantity. Therefore, a huge number of variants of plasma processes were developed. Additionally, a series of other synthesis process are connected to plasma, even when they are usually not referred as plasma process. Some of these processes are discussed within this article, too.

Langmuir (1928) coined the notation plasma in 1928. It describes a gaseous state of matter containing electrically charged particles; where the sum of these charges is nil. The charged particles may be electrons, ionized atoms or molecules, and, in case of synthesis processes, charged nanoparticles. As the charge carriers are mobile, plasmas show electric conductivity. It is important that the degree of ionization, the ratio of charged particles over the neutral ones, may be quite small. A plasma containing particles is called "dusty plasma"; therefore, plasmas used for particle synthesis are always dusty ones. With respect to synthesis, one distinguishes between plasmas at low and at high pressure.

D. Vollath (✉)
NanoConsulting, Primelweg 3, 76297 Stutensee, Germany
e-mail: dieter.vollath@nanoconsulting.de
URL: www.nanoconsulting.de

Particularly with regard to the classification of plasma processes, the differences between equilibrium and non-equilibrium plasmas are essential.

In an equilibrium plasma, the energy of all charged particles, often called temperature, is equal; whereas in a non-equilibrium plasma, electrons have the highest, the heavier ions a lower, and electrically neutral particles, the least energy. In view of plasma synthesis processes, this point needs detailed discussion. Flames are described as plasmas with low degree of ionization, sometimes called "low temperature partial plasma". In particle synthesis, the plasmas with the highest densities are observed in the plume of a laser focus. In view of precursors, one distinguishes processes using gases, solids, liquids or liquid solutions.

This is not the first review on plasma synthesis (See e.g. Szekely 1984; Boulos 1984; Heberlein 1989; Taylor and Vidal 1999; Manolache and Denes 2000; Kaneko et al. 2002; Vissokov et al. 2003). However, in contrast to earlier reviews, in this article, it was tried to give a consistent interpretation of the processes involved, in special, the influence of equipment design and operating conditions are taken into account. A major point, were, the conditions for self-limitating particle growth leading to monosized particles. A recent, more technically oriented review may be found in addition (Vollath 2007).

Energy transfer in plasma

Electrical fields transfer energy to charged particles. Particles with the charge Q passing an electrical potential difference V gain the energy

$$E = QV \tag{1}$$

In an alternating electrical field with the frequency f, the energy E transferred to charged particles with the mass m is

$$E \propto \frac{Q}{mf^2} \tag{2}$$

Equation (2) says that the transferred energy is proportional to the charge and inversely proportional to the mass of the particles and the squared frequency. This has important consequences, as the mass of the ions is a few ten thousand times larger than the one of the electrons. As a consequence, alternating electrical field transfer a significantly larger amount of energy to electrons as compared to ions or charged nanoparticles. The differences in the mass of the constituents of the plasma promote thermal non-equilibrium. Therefore, the "temperature" of the electrons is significantly higher than the one of the ions or neutral particles. Lastly, in non-equilibrium plasma, the definition of temperature is senseless. The "reaction temperature" is an average value determined at the exit of the plasma zone. The frequency in a plasma system may vary from the kilo-Hertz range in radio frequency (RF) to the giga-Hertz range in microwave systems. According to Eq. 2, in microwave systems, there are at least, six orders of magnitude less energy transferred to the charged particles as compared to RF systems; increasing frequencies favour low temperature systems.

In a plasma, however, the charged particles may not have the chance to get the whole energy of the electric potential, because they will collide with other particles in the plasma¸ therefore, the energy transfer is limited by the free path length or in other words, equivalent, by the collision frequency z. The collision frequency is proportional to the gas pressure. The energy transferred in plasma is: (MacDonald 1966)

$$E \propto \frac{Q}{mf^2} \frac{z}{+z^2} \tag{3}$$

Equation (3) shows the reduction of the energy transfer to the charged particles by collision with other neutral species. Figure 1 displays the relation between the transferred energy and the collision frequency.

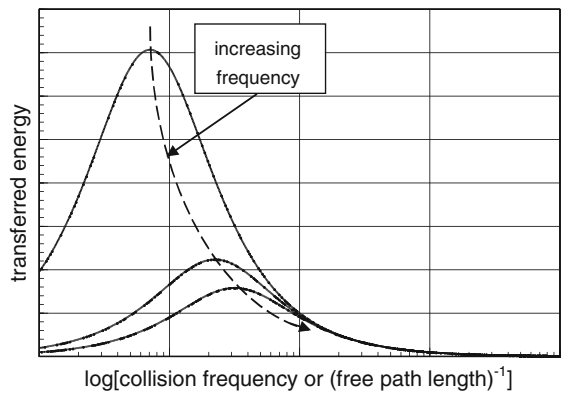

Fig. 1 Energy transferred in a plasma to charged particles as function of the collision frequency in the gas. With increasing frequency of the electrical field, the transfer maximum moves to higher collision frequencies and is less pronounced

The transferred energy goes through a maximum when the frequency of the electrical field is equal to the collision frequency. At high collision frequencies, the influence of the frequency of the electrical field vanishes. Experimentally, this case is observed at high pressure. On the other hand, as long as the collision frequency is smaller than the frequency of the electrical field, the charged particles gain the maximum possible energy from the electrical field. Therefore, one has to distinguish three possible cases with respect to the collision frequency:

- $z << f$: In this case, the energy of the electrons is sufficiently high to ionize the particles formed in the plasma. These conditions are observed at reduced gas pressure. As in resonant microwave cavities, the electrical field strength may be above 10^3 V cm^{-1}, the electrons gain enough energy to ionize the particles, whereas the probability for a recombination of the high energetic electrons with the ionized positively charged particles is small. As all particles carry positive charges, they repel each other. This phenomenon limits particle agglomeration (Vollath and Sickafus 1992a; Vollath and Szabó 2002, 2006).
- $z \approx f$: This intermediate case leads to particles carrying both positive and negative charges. Particles with opposite charges attract each other promoting particle agglomeration.
- $z >> f$: This condition limits the energy uptake of the electrons. The energy of the electrons is so small that they may attach at the surface of the particles. All particles carry negative electric charges; they repel each other. The size-limiting phenomenon occurs again (Mangolini et al. 2006). Matsui (2006) shows with model calculations, that, in this case the energy of the electrons is as low as 3 eV.

The exact limits between these three ranges depend from the gas pressure, frequency and field strength of the electrical field.

Experiments proof the influence of particle charges on agglomeration. Figure 2 displays a comparison between two zirconia powders synthesized in microwave plasma at reduced pressure. According to the discussion above, experimental conditions were selected in a way that the particles carried positive charges only. The product displayed in Fig. 2a was synthesized from $ZrCl_4$ (Vollath and Szabó 2006) in an argon oxygen mixture; in contrast, for the product displayed in Fig. 2b, water was added to the reaction gas. The water dissociated in the plasma, therefore, the following side reaction occurred:

$$\begin{aligned} &H_2O \Rightarrow H^+ + (OH)^- \\ &\text{particle}^{n+} + n(OH)^- \Rightarrow (\text{particle}^{n+} + n(OH)^-)^{\text{neutral}} \end{aligned} \quad (4)$$

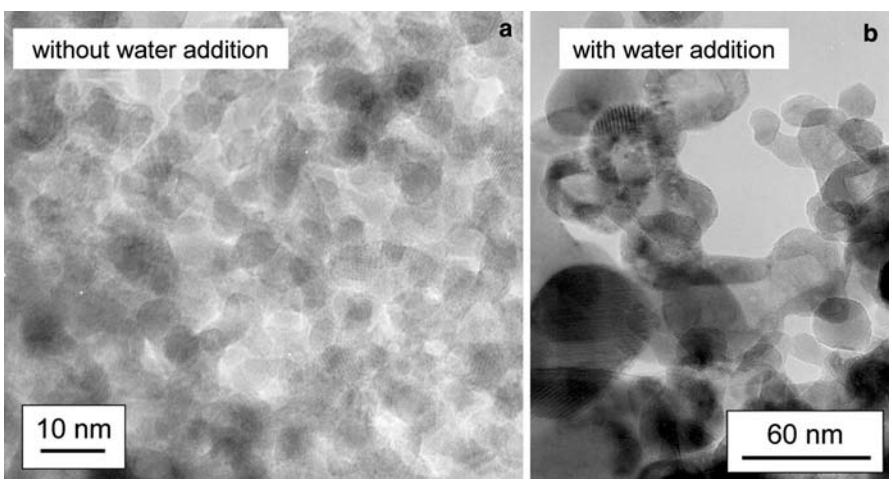

Fig. 2 Particle size distribution of zirconia synthesized in a microwave plasma (Vollath and Szabó 2006). (**a**) Product obtained under conditions, where the charge repulsion phenomenon was active. The particles are small; the size distribution is very narrow. (**b**) Product obtained under conditions, where the electrical charges of the particles were quenched by water additions. As the particles were not charged, the size distribution of the particles is very broad

Equation (4) shows that simply by adding water to the carrier gas, the positively charged particles are neutralized by collision with OH^- ions. As the particles are not longer repelling each other, one obtains a product with larger particles and broad size distribution.

The product displayed in Fig. 2a shows narrow particle size distribution; the average particle size is around 8 nm. The product synthesized with additions of water, as shown in Fig. 2b, is characterized by a broad distribution of particle sizes in the range from 10 to 50 nm. As an example for the case for negatively charged particles, Fig. 3 displays a particle size distribution of zirconia nanoparticles synthesized under conditions that led only to positively charged particles.

Except for a few isolated particles that are significantly larger, the particle size distribution depicted in Fig. 3 is remarkable narrow. Lastly, this is the consequence of the fact that the electrical charges of all particles carry the same sign.

Certainly, narrow particle size distributions are not per se an advantage. In some applications, such as sintering or as pigment, a broad size distribution may be better than a narrow one. Figure 4 displays a typical example for the particle size distribution of a product synthesized in a microwave plasma system not using the repelling phenomenon.

The particle sizes of the product, iron nanopowder, depicted in Fig. 4 are spread over nearly two orders of magnitude. This is a significant difference as compared to the characteristics of the products depicted in Figs. 2a and 3.

The question open until now is the dependence of the particle charge as function of the particle size. In a groundbreaking paper, Ziemann et al. (1996)

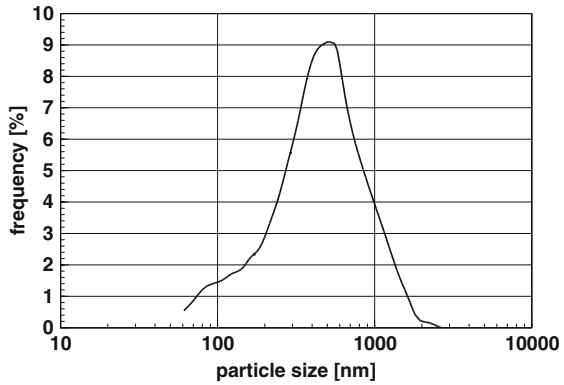

Fig. 4 Particle size distribution of iron nanopowder synthesized at atmospheric pressure in a microwave plasma. (Kalyanaraman et al.1998)

showed that for spherical particles, the electric charge increases linear with particle diameter. Deviations from linearity are attributed to significant differences of the radius of the curvature of the surface. Ziemann et al. (1996) performed these experiments using nanoparticles of three different oxides and a series of different sodium and potassium salts. Figure 5 displays experimentally well-based calculated particle charges as function of the particle diameter for FePt (Matsui 2006). Ziemann's linear relationship is confirmed again.

The linear relation between charges and diameter of the particles is understood readily: Considering a particle with the diameter D as spherical capacitor with the charge Q, the electric potential V at the surface is given by $V \propto Q/D$. As the charge Q of the particles increases linearly with the diameter D (See Fig. 5), the electric potential at the particle surface is independent of the size;

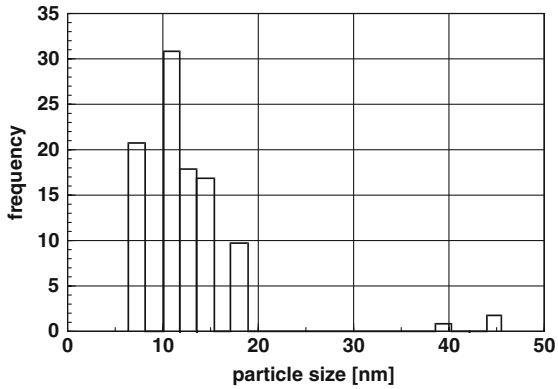

Fig. 3 Particle size distribution of zirconia made of zirconium butoxide in an AC plasma torch (Karthikeyan et al. 1997)

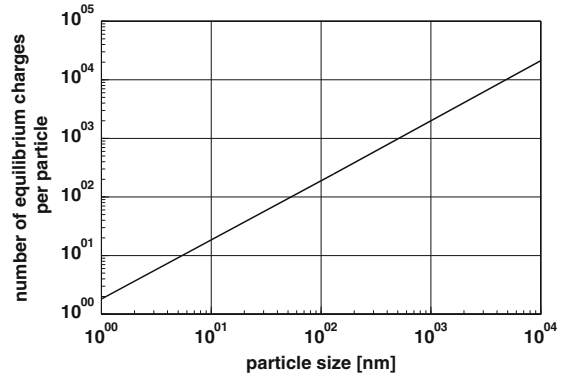

Fig. 5 Number of charges per FePt particle during synthesis in a RF plasma

Q/D is a constant parameter in the system. This is quite a simple explanation for the experimental findings.

In order to understand the mechanism of a reduction of the probability for agglomeration, Vollath and Szabó (2006) developed a simple model based on stochastic collisions. For neutral particles, this model calculates the collision probability $p_{1\text{-}2}$ for two particles with the diameters D_1 and D_2:

$$p_{1-2} \propto (D_1 D_2)^{0.5} \tag{5}$$

The term $(D_1D_2)^{0.5}$ called "collision parameter" increases with increasing particle size.

Particles with charges of equal sign repel each other; the repelling force is proportional to Q_1Q_2. This repelling force leads to a reduction of the collision probability (Vollath and Szabó 2006). Taking $Q \propto D$ into account, one obtains:

$$p^*_{1-2} \propto (D_1 D_2)^{0.5} \frac{1}{D_1 D_2} = (D_1 D_2)^{-0.5} \tag{6}$$

In contrast to Eq. 5, the particle size dependent collision parameter for charged particles $(D_1D_2)^{-0.5}$ decreases with increasing particle size.

Comparing Eqs. 5 and 6, teaches how to design gas phase synthesis systems with respect to optimal particle size distribution. Equation (5), valid for uncharged particles, says that the collision probability, and therefore, the probability for agglomeration, increases with increasing particle diameter. Lastly, this is the reason for the broad non-symmetric particle size distribution with an extended tail on the side of the large particles that is well described with a log-normal distribution function.

As the electrical charge increases with increasing particle diameter, situations where particles carry electric charges of both signs enhance agglomeration. However, in case that all particles carry charges with equal sign, Eq. 6 teaches that the probability for collision decreases with increasing particle size. This phenomenon limits particle growth in plasma processes. Additionally, that is the reason why it is nearly impossible to produce nanopowders with sizes outside of a narrow range, when the particles carry electric charges of equal sign. In cases, where the precursor fragments are highly ionized, any particle formation may be thwarted.

In this context, it must be shown that Ziemann et al. (1996) also found the following possibility for the particle size dependency of electric charges:

$$\begin{aligned} D < D_c &\rightarrow Q = 1 \\ D > D_c &\rightarrow Q = 1 + \alpha(D - D_c) \end{aligned} \tag{7}$$

Certainly, Eq. 7 is based on the quantized nature of electric charges. The consequence of Eq. 7 is, that up to the critical particle diameter D_c, the collision probability increases, whereas, it decreases for larger particles, according to Eq. 6. The collision parameter exhibits a maximum at the critical particle diameter D_c. Even when electric charges are quantized, these steps are not observed experimentally, because experimental results describe the average of many particles levelling out these steps.

Design of plasma systems for nanoparticle synthesis

General considerations

Devices for plasma synthesis may be grouped by temperature, gas pressure, frequency or the existence of electrodes or not. Fundamentally, one finds high temperature processes, where temperatures significantly above 1,000 K are observed and low temperature processes with temperatures below 1,000 K. In most cases, high temperature processes are connected to higher gas pressures as compared to low temperature processes working at reduced gas pressure. Except for a few very special designs, low temperature processes are not using electrodes. Figure 6 displays the general layout of a system for plasma synthesis.

The important and environmentally friendly point of gas phase synthesis processes using plasma is the small amount of effluents. Just the reaction products stemming from the dissociation of the precursors

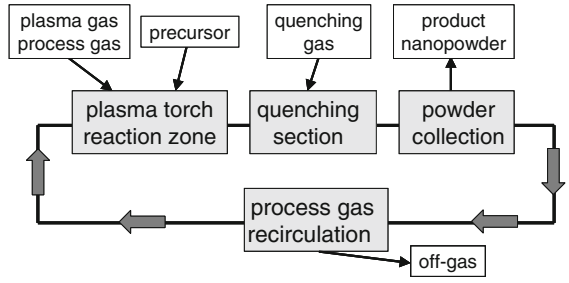

Fig. 6 General lay-out of a powder production system based on a plasma system

have to be removed from the system. In an industrial equipment, all the other process gases are recirculated. However, this statement is valid only for the synthesis process itself. The relations may be different if the production of the electric energy is taken into account. Recirculation is of special importance, e.g. in the synthesis of nitrides, where pure nitrogen or nitrogen/ammonia mixtures are used for nitriding or for metal carbide synthesis, where argon is used as carrier gas.

Particles are moving randomly in the plasma. Additionally, they have a drift movement in the direction of the gas stream. Therefore, there is a high probability for collision of the particles in the plasma. This is the reason for cluster formation, leading to broad particle size distributions. This adverse effect is reduced by a well-designed efficient quenching step directly after the plasma zone. Quenching gas is introduced either radially or axially against the flow direction into the system. Quenching is necessary only in high temperature processes; low temperature processes do not need quenching.

Quenching influences product quality significantly. Figure 7 displays the morphology of GeO synthesized in a RF plasma device, as function of the quenching conditions (Tekna Plasma Systems Inc. 2007).

Figure 7 demonstrates, just by increasing the flow of the quenching gas, it is possible to reduce the width of the particle size distribution significantly. From the conditions with low quenching gas flow, as displayed in the left micrograph, where the particle size ranges from 30 to 500 nm, the particle size is reduced and the distribution narrowed to a range from 30 to 100 nm, in case of maximal quenching gas flow. This particle size reduction is observed as increased BET surface, too. This example demonstrates the importance of selecting proper conditions for quenching in high temperature processes. It is important to realize that, in most instances, the main difference between unquenched and quenched products is found in the tail on the large particle side of the size distribution. The size distribution of the largest part of the particles is more or less not influenced (Goortani et al. 2006).

In following text, plasma processes are grouped according to the frequency of the supply of electrical energy. Therefore, it will be distinguished among DC, AC and RF systems as first and microwave systems as second group.

DC, AC and RF systems using electrodes

Plasma processes obtaining their electrical energy from DC, AC or RF sources are the oldest and most common ones. In most cases, they are operated at atmospheric pressure; therefore, operating temperatures are very high. Under these conditions, the plasma is not too far from thermal equilibrium. One observes temperatures significantly above 4,000 K; (Rao et al. 1999, Kim 2005) temperatures, where all of the metals and most of the oxides applied as precursors are evaporated, at least melted. Therefore, one observes no correlation between the sizes of the precursor particles and the size distribution of

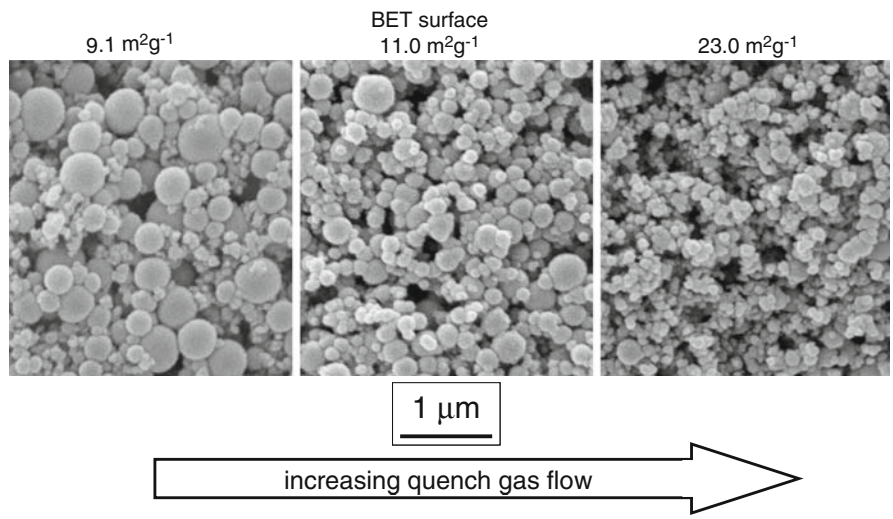

Fig. 7 GeO powder synthesized in a RF plasma torch. The micrographs show the influence of the quenching conditions on particle size, here expressed as BET surface (Tekna Plasma Systems Inc. 2007)

particles in the product. As these processes operate at atmospheric pressure, they are characterized by bipolar charged particles. Therefore, one has to expect relatively broad particle size distributions in the product. Figure 8 displays two of the most common designs using electrodes.

In both designs depicted in Fig. 8, plasma is burning between two co-axial electrodes. In the concentric space between the electrodes, process and carrier gases are supplied to the system. This powerful gas stream blows the plasma out of the electrode system; a plasma torch is formed. Additionally, this gas cools the electrodes. However, it may be necessary to cool the electrodes with water, too. The precursor is admixed to the system either axially in a centre bore of the inner electrode or outside of the electrode system perpendicularly to the plasma torch. The precursor may be solid, liquid, or, in rare cases, gaseous. Liquid precursors are either suspensions, aqueous or organic solutions. In case of oxide synthesis from liquid organic solutions, the energy content of the plasma flame is increased significantly.

In case of axial feed of the precursor, depositions of reaction products at the orifice may lead to clogging. This is reduced by a powerful stream of gas in the space between the electrodes and sheath

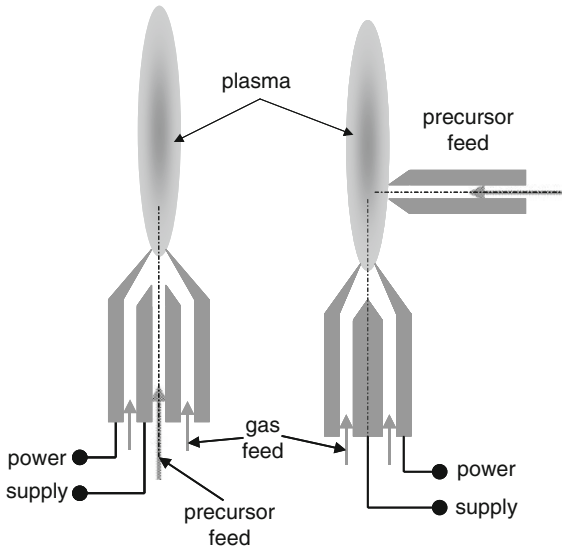

Fig. 8 Basic designs of plasma burners for nanopowder synthesis using electrodes. The designs differ in the supply for the precursor. Both designs allow the use of liquids or powders as precursor

gas circumferentially to the nozzle system. In most cases, the systems are designed in a way that makes transport pumps for the precursor superfluous. Feeding the precursor perpendicular into the plasma torch is, at most, applied for powders only. The design of the nozzle is the crucial point with respect to product quality. Nozzle design reach from very simple to highly sophisticated ones with hypersonic gas velocities (Rao et al. 1999; Kim 2005).

Typically, products obtained by plasma nozzle processes are highly agglomerated (Cruden et al. 2003; Cota-Sanchez et al. 2005; Marzik et al. 2005; Tong and Reddy 2005; Wang et al. 2005; Ko et al. 2006). Very careful selection of the synthesis parameters may lead to products with remarkable narrow particle size distributions. Karthikeyan et al. (1997) produced zirconia nanopowder using 2.4 wt.% zirconium butoxide dissolved in *n*-butanol as precursor. Interestingly, the dissolved precursor was injected radially into the plasma torch. As shown in the particle size distribution (Fig. 3), the average particle size of this product is around 12 nm. Besides the majority of particles of nearly equal size, only a few larger particles are observed. Kim (2005) described a special design using ablating electrodes. This author produced AlN from an electrode made of metallic aluminium in a 50/50 vol% nitrogen/ammonia atmosphere. The necessary high plasma temperature was obtained using a pulsed DC source. The nozzle itself was designed to obtain hypersonic gas velocities.

Devices for powder synthesis, as described above, are widely used and mature in its design. It is possible to purchase systems of different sizes ready for use. Therefore, the most important technical details are, because of their huge technological relevance, kept in secret and not published in open literature. Designs as depicted in Fig. 8, may be used for plasma coating, too.

RF systems

Inductive coupled systems

RF systems for plasma synthesis of nanopowders are, in general, designed as electrode-less systems. The advantage of these systems is that there is no risk to obtain impurities from the electrodes. On the other hand, consumable electrodes as precursors are

excluded. The range of frequencies applied in such systems reach from 50 kHz up to 10 MHz. Figure 9 displays the typical layout for a RF plasma device for nanopowder synthesis. It consists of a nozzle system for the supply with precursor, reaction and carrier gas, which is similarly designed as the one for ones using electrodes. The main difference is the inductively coupled plasma.

As shown in Fig. 9, in most cases, the precursor is supplied axially. A further design uses an arrangement with opposite flow direction of plasma gas and precursor. (Schulz and Hausner 1987, 1992; Goortani et al. 2006) The advantage of the latter design is, according to the authors, the extended period of time, where precursor and plasma are in contact. Certainly, there is an advantage in cases, where the reaction rate of particle formation is extremely low. Similarly, as in the case of electrode systems, quenching of the product directly after the reaction zone improves product quality.

Also for electrode-less systems for powder synthesis, turn-key industrial systems are readily available. The capacity of these systems reaches from gram to kilogram per hour (e.g. Tekna Plasma Systems Inc. 2007). A typical example for a product of such an industrial equipment is shown in Fig. 10. Tekna Plasma Systems Inc. (2007) displays metallic nickel powder with an astonishing narrow particle size distribution. Some of the particles with non-spherical shapes show clearly that they were melted before agglomeration.

Highly optimized industrial systems produce nanopowders of good quality with particle sizes of <100 nm. The range of possible products covers metals, oxides, carbides and nitrides. Except for

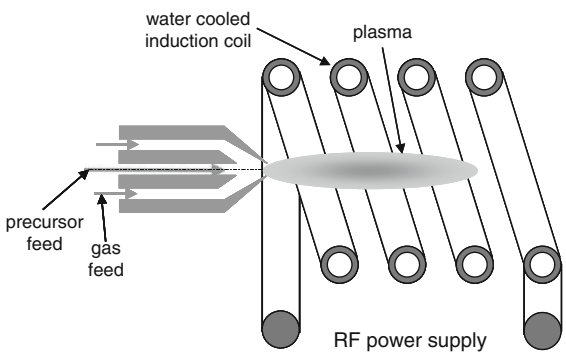

Fig. 9 General design of RF synthesis equipment with inductively coupled plasma

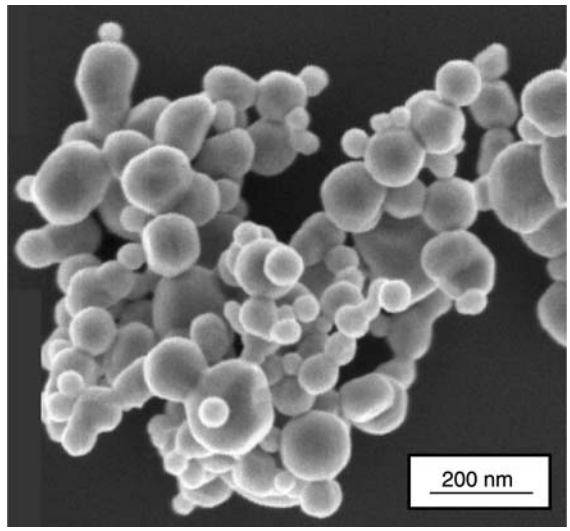

Fig. 10 Nickel powder made by an industrial RF plasma process (Tekna Plasma Systems Inc. 2007). The shapes of the agglomerates clearly indicate that the particles were melted during agglomeration

oxides and precious metals, powders of these products may be highly pyrophoric. Therefore, it is advised to handle these products in an inert gas atmosphere, if possible within glove boxes.

A few further more recent applications of powder synthesis applying RF plasma torches, outside of industrial use, are found in articles of Grabis et al. (1998), Mohai et al. (2001), Son et al. (2003), Szépvölgyi et al. (2004) and Castillo and Munz (2005).

Capacitive coupled systems

A series of capacitive coupled systems was built for the synthesis of nanopowders. Also in this case, there are designs applying electrodes or electrode-less systems. A large variety of designs work with pulsed RF plasma using a design similar as displayed in Fig. 11 (Matsui 2006; Schweigert and Schweigert 1996; Kortshagen and Bhandarkar 1999).

Within a reaction tube, two gas permeable electrodes characterize the design depicted in Fig. 11. It is possible to adjust the gas pressure in a way that there are only unipolar charged particles in the system (Matsui 2006). Therefore, the synthesis of products with quite a narrow particle size distribution is possible. The pulse length for the systems as depicted in Fig. 11, ranges from a few tenths (Buss

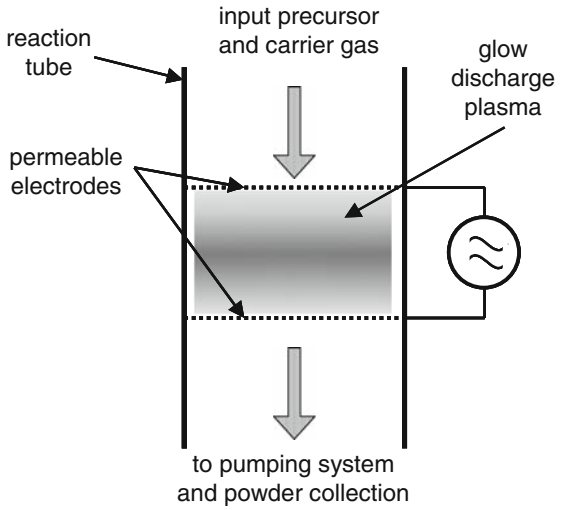

Fig. 11 Capacitive coupled RF system to synthesize nano-powders using a pulsed source of energy. When power is "on" the particles, kept in between the permeable electrodes, are nucleated and grow. During the "off" time, the particles are transported out of the reaction zone (Matsui 2006)

1997) up to 30 s (Matsui 2006). With increasing time, the average size of the particles increases. By proper adjustment of the precursor supply, this allows quite a precise control of the particle size. Figure 12 displays typical examples of the growth of the particle size with pulse length.

Matsui (2006) shows the synthesis of FePt, a hard magnetic, intermetallic compound. For both constituents, organic precursors were used. There was a steady flow of gas through the reaction zone, which is the space between the two permeable electrodes. As long as RF power was on, the particles stayed in the reaction zone and grew. After switching RF power "off", the particles were moved out from the reaction zone and collected. Gas pressure and frequency were selected in a way that particles carried negative electric charges only. Therefore, the resulting particle size distribution was narrow. As shown in Fig. 5, the electric charges increased linearly with the particle diameter. In contrast, because of different operating conditions, the product, silicon ex silane, obtained by Buss (1997) showed a broad particle size distribution.

Capacitive coupled systems are possible in electrode-less design, too. Figure 13 displays the general layout of such a design.

In order to avoid too high temperatures, it is necessary to operate at relatively low gas pressure. Therefore, the gas pressure is selected to be in the range between 0.1 and 1 mbar. This low gas pressure limits the production rates significantly. However, there are reports that such systems are well suited for highly specialized materials. Anderson et al. (1989) synthesized successfully complex oxides, such as spinelles or high temperature superconductors, and silicon nitride. Provided it is possible to avoid condensation of the reaction product on the walls of

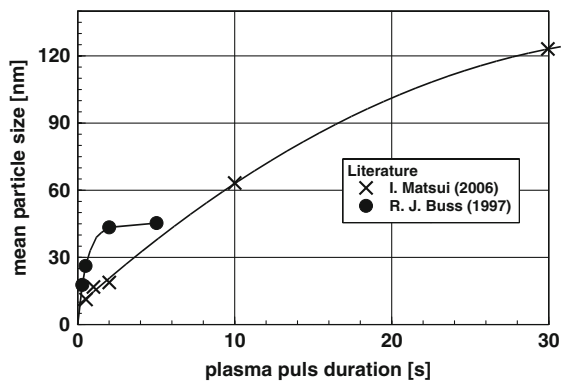

Fig. 12 Influence of the "Power ON Time", the plasma pulse duration, in an equipment according to Fig. 11 on the mean particle size of the product (Matsui 2006, Buss 1997)

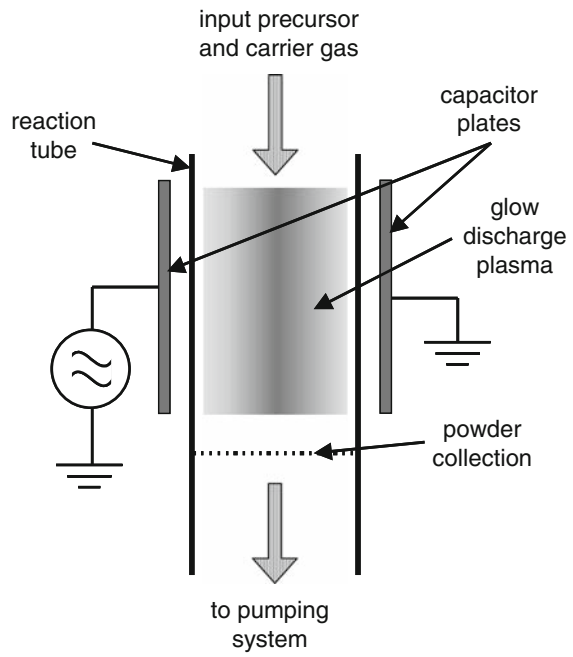

Fig. 13 Design of an electrode-less capacitive coupled reactor for powder synthesis using a RF power source (Anderson et al. 1989)

the reaction vessel, it is possible to produce metallic particles, too.

Microwave systems

Low-pressure systems

In view of design simplicity, product quality and universal application, microwave systems working under reduced pressure are unmatched. The first successful system was set-up by Vollath and Sickafus (1992a), Vollath and Szabó (2002). Figure 14 displays the basic design of a low-pressure microwave system.

Such a system consists basically of a resonant microwave cavity connected to a wave-guide to supply the system with microwave energy. Successful realizations apply the industry frequencies 0.914 and 2.45 GHz. Resonant cavities applying the TE_{01} (Vollath and Sickafus 1992a) or a rotating TE_{11} (Vollath and Szabó 2002) mode were realized. Experience taught, higher frequencies, leading to smaller plasma zones are of advantage with respect to product quality without loss of output (Vollath and Szabó 2002, 2006). The design, displayed in Fig. 14, is characterized by a reaction tube passing the TE_{11} resonant microwave cavity. At the entrance and exit points of the cavity, a cut-off tube is attached. This tube reduces the intensity of the leaking microwaves to a tolerable level. During synthesis, the evaporated precursor, transported by carrier and reaction gases, is flowing through the reaction tube. As reaction gas, one applies a mixture of argon with oxygen for oxide synthesis or nitrogen with ammonia for nitride synthesis. It is important that the carrier gas is properly heated, otherwise, the precursor condensates during the transport, leading to unintended large particles. At the intersection between the microwave cavity and the reaction tube, plasma is ignited. The gas pressure in the system can be adjusted in a way that the energy of the electrons is in the range of keV or only a few eV. Most successful is the operation at reduced pressure, where the free path length of the electrons is large and, therefore, the energy of the electrons high. These highly energetic electrons ionize the particles. Therefore, during synthesis, all particles carry positive charges, they repel each other; as a result, the particles are not agglomerating during synthesis. These well-separated particles of nearly equal size are very well visible in Fig. 2a, where zirconia particles are depicted. Keeping the residence time of the particles in the plasma short improves the product. Usually, the velocity of the gas flow is selected to limit the dwell time of the particles in the reaction zone to the range between 5 and 10 ms.

A typical nitride, synthesized in microwave plasma at reduced pressure is depicted in Fig. 15 (Vollath and Sickafus 1992b, unpublished results), 1993).

The product displayed in Fig. 15 excels in uniform particles, which is typical for this kind of products. Also Shimada et al. (2006) synthesized GaN successfully in a system using a resonant microwave cavity of different design, with similar good success.

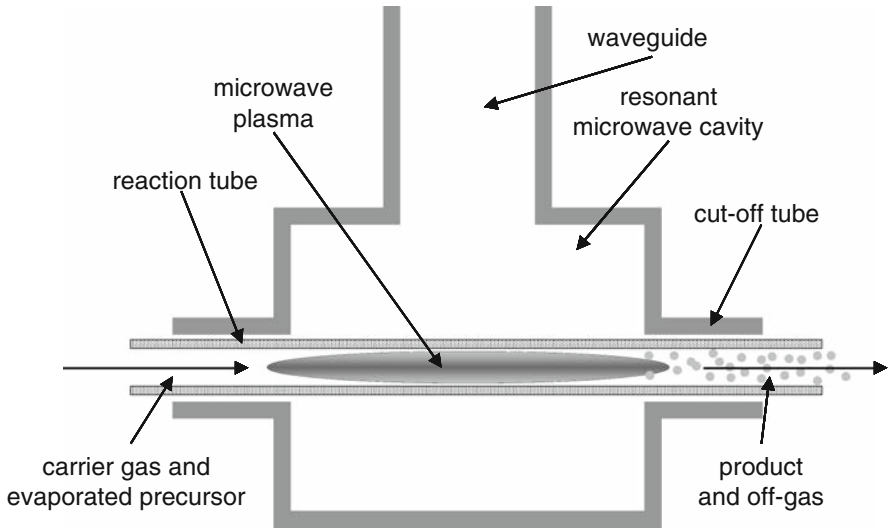

Fig. 14 Microwave plasma system working at reduced pressure. (Vollath and Sickafus 1992a; Vollath and Szabó 2002) The cut-off tube, an important feature of the microwave design, is necessary to avoid leaking of microwaves outside to the environment

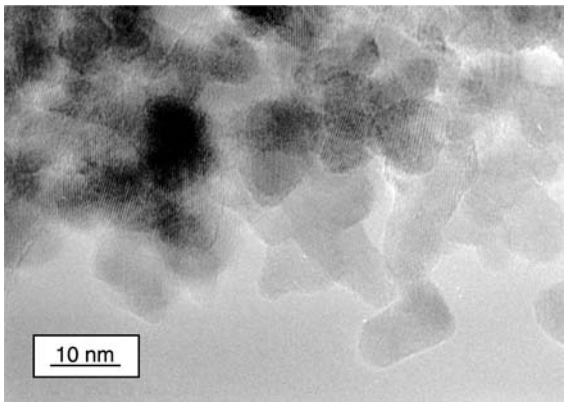

Fig. 15 Zirconium nitride powder synthesized in a microwave plasma device. Obviously, the size limitation due to particle charging works in case of nitride synthesis, too (Vollath and Sickafus 1992b, unpublished results)

Besides these more conventional products as oxides or nitrides, compounds with layered structures, such as sulphides or selenides were synthesized, too (Vollath and Szabó 1998, 2000). Figure 16 shows a typical example for this kind of products. This figure displays an electron micrograph of tungsten sulphide, WS_2. For the synthesis of sulphides, H_2S was chosen as source for sulphur. Interestingly, because of the short residence time in the reaction zone, most of the particles did not form fullerene-like shapes or nanotubes. The formation of these structures takes more time (Feldman et al. 1996; Zak et al. 2000).

There are further possibilities to exploit the repelling phenomenon of particles with charges of equal sign. In this context, the most interesting application is the synthesis of coated particles. Coating of nanoparticles expands the possibilities for application. Such coatings may act as distance holder to reduce interaction of the particles; a feature important, e.g. for magnetic particles, or, what is even more interesting, coatings allow to combine different properties in one particle. A typical example is the combination of ferromagnetism and luminescence (Vollath and Szabó 2004, 2006). However, even with a low-pressure microwave system, coating of particles is not a simple task, because the particles loose parts of their electrical charge on the way between these two reaction stages, resulting in some clustering of particles. Therefore, the coating step following the synthesis of the kernel must be as close as possible. Otherwise, coating of individual particles is impossible. The coating itself may be a second ceramic material, a polymer, or any other organic or inorganic compound.

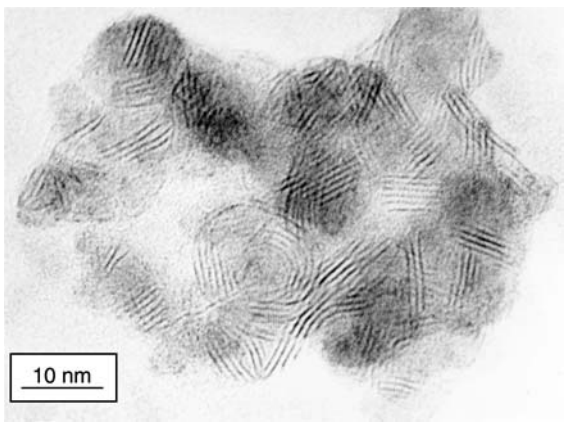

Fig. 16 Tungsten sulphide synthesized in a microwave plasma device (Vollath and Szabó 1998)

Figure 17a displays the design for the synthesis of particles with a ceramic coating (Vollath and Szabó 1994). Two identical cascaded microwave cavities, the first one for synthesis of the core and the second one for coating, characterize such a system. The length of the cut-off tubes determines primarily the distance between these two cavities. Setting the system into a microwave tight box avoids this problem and improves the quality of the product. In order to obtain coatings of organic materials, the second step consists essentially of a conventional furnace, as it is depicted in Fig. 17b. In this case, the considerations with respect to the length of the cut-off tube are valid, too. It must be noted, synthesis of coated particles is not restricted to one layer. There are equipments for ceramic double layer systems (Vollath and Szabó 2002) or for two organic layers, such as an organic lumophore as first layer and a polymer as second one (Vollath and Szabó 2000).

Figure 18a and b display examples for ceramic particles coated with a second ceramic phase (Fig. 18a) and a polymer phase (Fig. 18b). It is important for the application, and characteristic for the stochastic process of coating, that the thickness of the coating is equal at any point of the convex surface.

Systems operating under ambient pressure

Generally, processes working under reduced pressure are more expensive compared to those working under

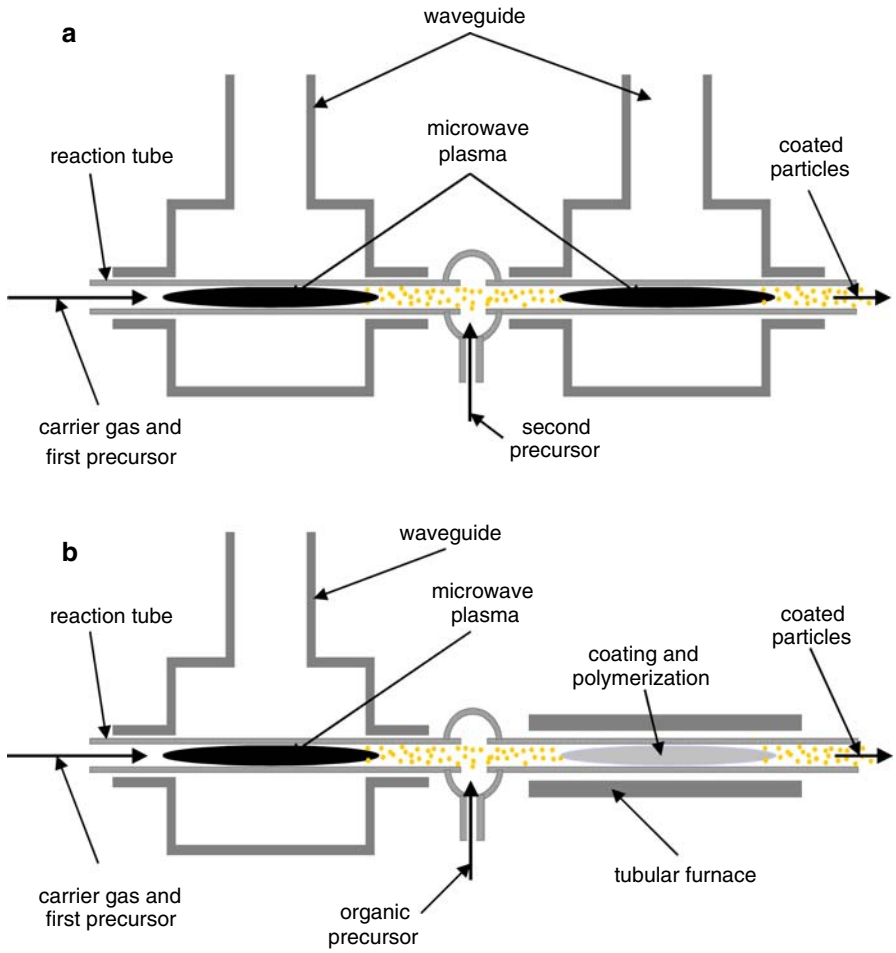

Fig. 17 Arrangements to produce coated nanoparticles. (**a**) Device to produce ceramic coated ceramic particles (Vollath and Szabó 1994). (**b**) Device to obtain polymer coated ceramic particles (Vollath et al. 1999). Additionally, it is possible to use other organic compounds, like lumophores, as coating (Vollath and Szabó 2004)

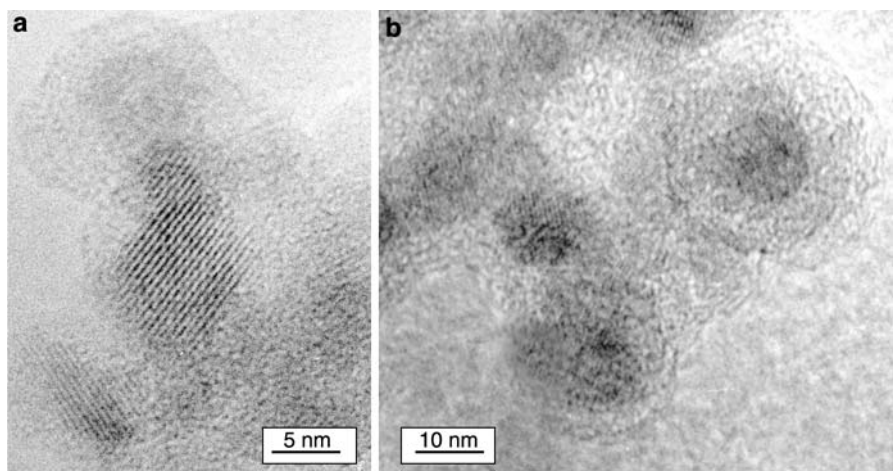

Fig. 18 Typical examples of nanoparticles coated in the microwave plasma process operating under reduced pressure (Vollath and Szabó 1994; Vollath et al. 1999). (**a**) Zirconia particles coated with alumina. (**b**) Iron oxide particles coated with PMMA

ambient pressure. In special, because of the pressure-loss in filter systems, particle collecting is more difficult in low-pressure systems. These are important arguments to develop processes working under ambient pressure. However, also in microwave systems for powder synthesis, the temperature is higher as compared to systems working under reduced pressure. A typical design for a microwave system

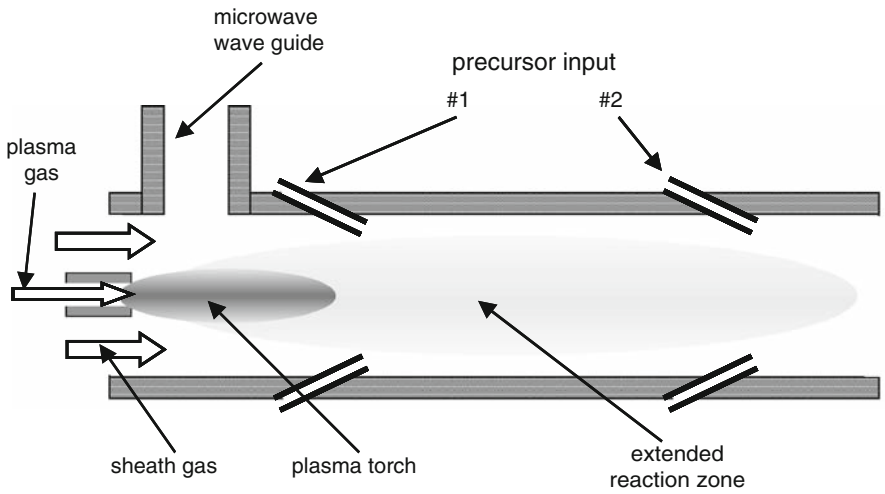

Fig. 19 Microwave plasma system working under ambient pressure. Two consecutive inputs for precursors allow synthesis at different temperature levels or the production of something like coated nanoparticles

working under ambient pressure is depicted in Fig. 19 (Brenner et al. 1997; Kalyanaraman et al. 1998; Troitskiy et al. 2003; Chau et al. 2005, 2006).

This design applies a microwave plasma torch. In a certain distance after the plasma torch, the precursors are introduced. The reaction temperature is adjusted by the distance of the precursor input to the end of the plasma torch; with increasing distance, the temperature gets lower. Additionally, multiple inputs for the precursor allow the production of something like coated nanoparticles (Chau et al. 2006). As these systems work at atmospheric pressure, the mean free path length of the electrons is small; therefore, within the reaction zone, after the plasma torch, number and energy of the remaining electrons is small. As a result, particle charging and repulsion are poor. Like in all other processes working at ambient pressure, the products are highly agglomerated with broad particle size distribution. (Chau et al. 2006) The particles obtained, range from fine fuzz to large facetted particles with diameter up to nearly 40 nm. A typical size distribution of such a product, iron nanoparticles, is displayed in Fig. 4 (Kalyanaraman et al. 1998).

These products must not be compared with those stemming from the low-pressure microwave process. In a more realistic comparison with RF processes working under ambient pressure, the products are more or less comparable. In this context it is important to mention that—at least in the range of low power systems—microwave systems are significantly cheaper than those working in the RF range.

Other plasma processes

Laser processes

Plasma processes driven by laser excel in extreme high dense plasmas, concentrated in the small volume of the laser focus. Therefore, to obtain products with sufficiently low agglomeration, it is necessary to remove the product as fast as possible from the reaction zone. Laser processes may be divided into two major groups:

- Laser processes with gaseous targets and
- laser ablation processes with solid targets.

The laser process, most similar to the ones that are described in the previous chapters, works with a gas target. As it is depicted in Fig. 20, successful designs of laser gas phase synthesis are characterized by the focus of the laser directly above the orifice, where the gaseous precursor and the reaction gas enter, already premixed, the reaction vessel. Above the orifice, in the laser focus, plasma is formed. In this plasma, the concentration of reactants is extremely high. Therefore, the tendency to form agglomerates is typical for this process. Generally, the reaction product is highly agglomerated; (Morjan et al. 2003) in many instances it forms chains. If necessary, a carrier gas is added to remove the reaction products as fast as possible out of the reaction zone. Figure 20 displays the general layout of a laser system working with a gas target.

As the supply of high intensity energy is most cheap with IR CO_2 lasers emitting at 10.6 μm, additions of IR absorbing gases, sensitizers, like

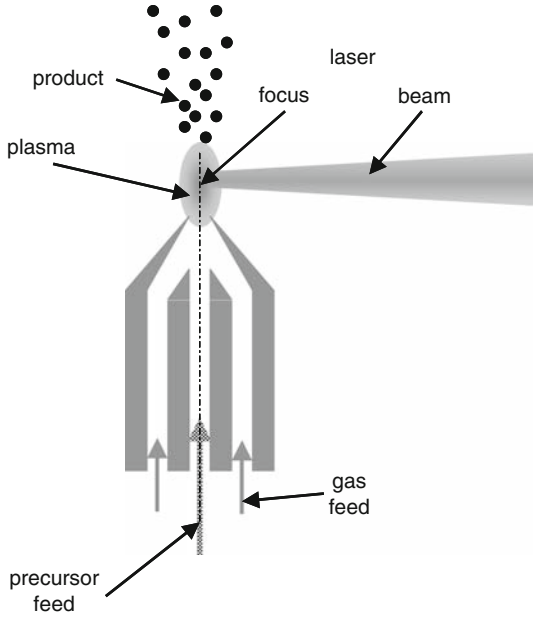

Fig. 20 System for nanoparticle synthesis using a laser-driven plasma with a gaseous target

SF_6 or C_2H_2 (Morjan et al. 2003; David et al. 2004; He et al. 2005) are necessary. Additions of sensitizers may have adverse effects, too. In special, the application of SF_6 may lead to the formation of unwanted fluorides as by-products. (He et al. 2005) On the other hand, these unavoidable side reactions may be used to obtain very special products. David et al. (2004) synthesized α-Fe particles embedded in graphite using $Fe(CO)_5$ as precursor, C_2H_2 as carrier gas and SF_6 as sensitizer. However, it is necessary to remark that this product was entirely different as compared to coated particles as reaction rate and particle density in the plasma were high. The carbon needed for the embedding graphite originated from the C_2H_2, dissociated in the laser plasma.

The second laser driven plasma process applies solid targets. In this case, the laser ablation process, the intensity in the focus is so high that the solid target is evaporated and the emerging gas is ionized. This plasma is responsible for the further progress of the reaction leading to particle synthesis. From the many systems described in literature, it is possible to extract a few characteristic design features, displayed in Fig. 21.

The laser target, the precursor, may be metallic, ceramic or any complex mixture. Due to the high energy density in the laser focus, any material in the laser focus evaporates immediately; therefore, also in case of complex targets, the stoichiometry of the target is preserved. The processes in the laser focus are quite complex. The evaporated material leaves the surface of the target perpendicularly in a plume. The intense electrical field of the laser ionizes the material in the plume. The temperatures in the plume reach 3,800 K (Puretzky et al. 2000) or more. During adiabatic expansion of the plume, the temperature is reducing. After the decreasing temperature has reached the level of supersaturation, nuclei are formed; the particles start to grow. The expansion rate of the plume increases with decreasing gas pressure in the system. The expansion of the plume limits particle growth. Hence, one may expect

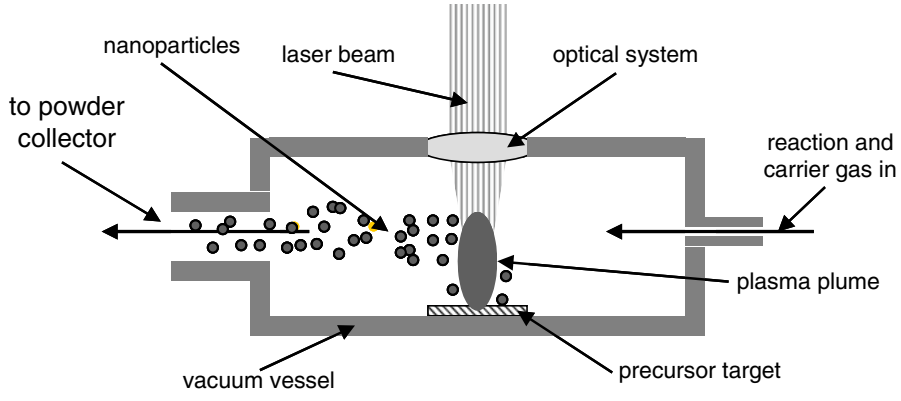

Fig. 21 General layout of an experimental device for powder synthesis applying laser ablation. The pulsed laser beam is focused at the surface of the precursor, the target, metal or oxide, and evaporates it. A plume, a supersonic jet of evaporated material, is ejected perpendicular to the target surface. In the plume, particles are formed. The carrier gas containing reactive gas components transports these particles to the powder collector

decreasing particle size with decreasing gas pressure. On the other hand, in cases of high gas pressures, one may expect decreasing particle sizes with increasing pressure, because in the slower expanding plume, the supersaturation remains a longer time, giving a chance for the formation of an increased number of nuclei. Both phenomena are observed. Actually, there is an interaction of both mechanisms leading to a complex dependency of the mean particle size of the gas pressure. Figure 22 displays the dependency of the mean particle size of Co_3O_4 made of a rotating target of the same composition in argon atmosphere. An ArF excimer laser with 17 ns pulse length was used as energy source (Li et al. 1999).

The experimental results depicted in Fig. 22 confirm the considerations on nucleation and particle growth as function of the gas pressure. In fact, one finds the smallest particles at the lowest and the highest gas pressure. In-between, there is a bimodal maximum. However, caused by the high particle density in the plume, the particles are not isolated ones, rather, they appear in chains or other agglomerates. Selecting the process conditions properly, allows reducing the degree of agglomeration.

Particle formation and growth in the plume are random processes; therefore, broad asymmetric particle size distributions are expected and found experimentally. Figure 23 displays such a particle size distribution determined on a γ-Fe_2O_3 specimen (Wang et al. 2006). In the pressure range above 2 * 10^5 Pa, also these authors found decreasing particle sizes with increasing gas pressure.

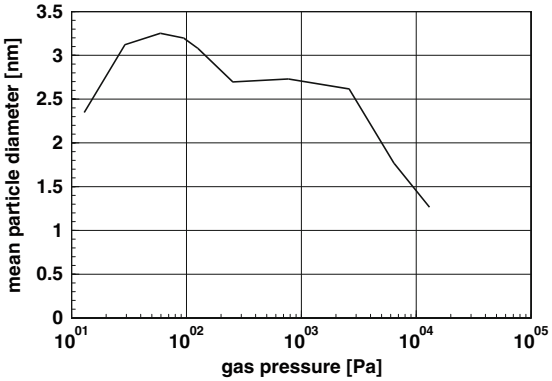

Fig. 22 Average diameter of Co_3O_4 particles produced from a target with identical composition in argon atmosphere by the laser ablation process. The smallest sizes of the particles are observed at the lowest and highest gas pressure. An ArF excimer laser was applied as energy source (Li et al. 1999)

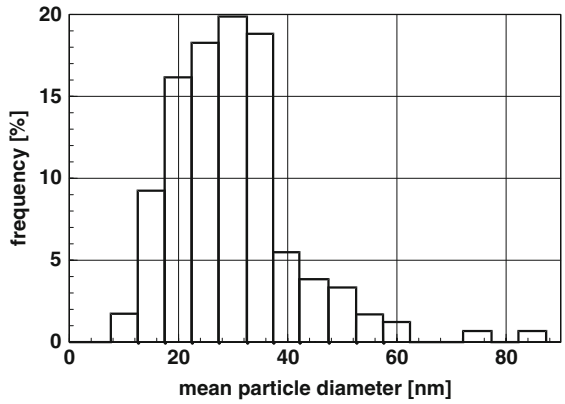

Fig. 23 Fe_2O_3 particles produced by the laser ablation process. Please realize the relatively broad size distribution, which is typical for laser ablation processes working under ambient pressure (Wang et al. 2006)

Flame processes

Flames are often considered as "partial plasmas". This is, due to thermal ionization, flames contain a certain amount of ions and free electrons. There are many possibilities to exploit this phenomenon. It is possible to increase flame temperature with microwaves or one can separate charge carriers using a DC field across the flame. Until now, there is only one group trying systematically to utilize this specific property of flames. Pratsinis (1998) and Kammler (2002) added an electrical DC field across flames and studied the influence on the product. Figure 24a depicts a schematic drawing this design consisting of two plates, connected to a DC voltage directly above the orifice of a burner system; Fig. 24b displays a photograph of the actual experiment.

Figure 24b clearly shows that the electrical field of less than 2 kV cm^{-1} splits the flame and draws the particles out of the flame. These particles are deposited on both electrodes indicating that particles are carrying electric charges of both signs. The amount of particles of either sign is nearly equal. Pulling the particles with an electrical field out of the flame has two advantages: (i) The agglomeration of particles is significantly reduced as particles of equal sign have a reduced probability for agglomeration and (ii) the residence time of the particles in the flame is reduced, reducing particle growth and agglomeration, as well. These expectations are well confirmed by experimental results. Figure 25 displays the mean particle size of titania synthesized in a flame with transversal electrical

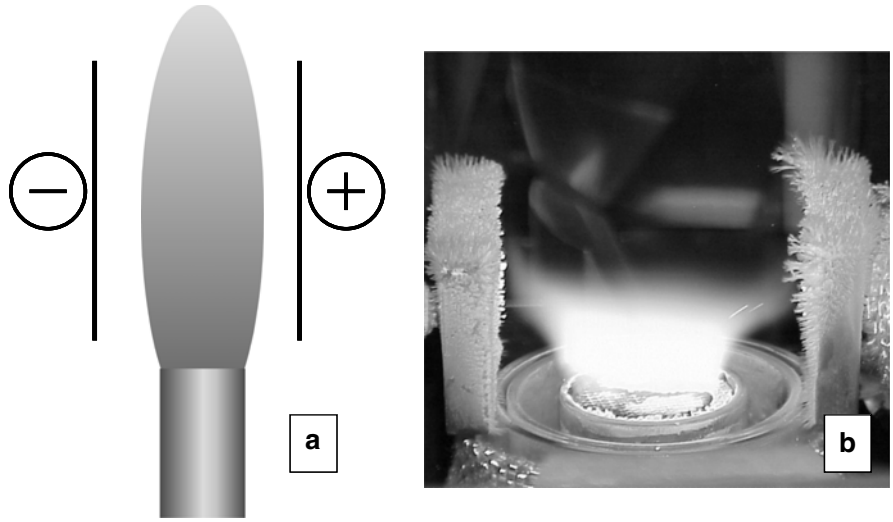

Fig. 24 Experimental set-up to synthesize nanoparticulate powders in flames using the property of a partial-plasma by applying an electrical field between plate electrodes transversal to the flame. (**a**) Design of the set-up. (**b**) Experimental realization of the design outlined in Fig. 25a. The figure shows a flame producing TiO_2 ex $TiCl_4$ in a methane–oxygen flame with transversal electrical field of <2 kV cm^{-1}. The electric field splits the flame. Electrically charged particles are attracted by the plate electrodes with different sign and deposited (Pratsinis 1998, 2006 (private communication))

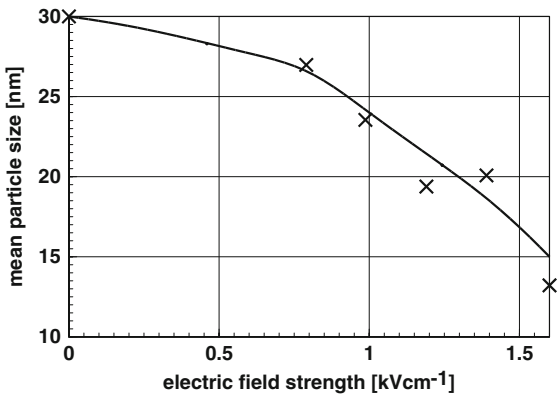

Fig. 25 Mean particle size of TiO_2 ex $TiCl_4$ synthesized in a methane–oxygen flame with a transversal electrical field. (Pratsinis 1998; Kammler 2002)

field. The effect of size reduction by the electrical field is obvious. Within these experiments, the electrical field strength was below 2 kV cm^{-1}. This field is so low that ionization by the electrical field is impossible; this makes clear that electrical charging of the particles must be attributed to processes in the flame.

In methane–oxygen flames, temperatures above 2,500 K are observed (Kammler et al. 2001). At these high temperatures, thermal ionization of gas molecules or particles will occur with high probability. Additionally, ionization of particles with free electrons, accelerated in the electric field, may occur. However, as the flame operates at atmospheric pressure, the free path length of the free electrons is small; therefore, their energy is relatively small, that is why attachment of free electrons at the surface of uncharged particles is possible, too. These processes lead to particles carrying electric charges of both signs that are separated in the electric field and move into the direction of the different electrodes. As a consequence, the tendency of agglomeration is reduced. These processes explain the experimental findings.

Due to the early extraction of the product from the flame, the particles are not only smaller, because of their reduced residence time in the flame, the chance for agglomeration is reduced; too; therefore, the particle size distribution is narrower. This is very well visible in the electron micrographs in Fig. 26, where TiO_2 ex $TiCl_4$ synthesized in a premixed methane–oxygen flame without (Fig. 26a) and with transversal electrical field (Fig. 26b) is depicted. The product obtained with transversal electrical field shows smaller particles and a narrower size distribution.

Conclusions

There is a wide variety of plasma processes applied for the synthesis of nanoparticulate powders. The

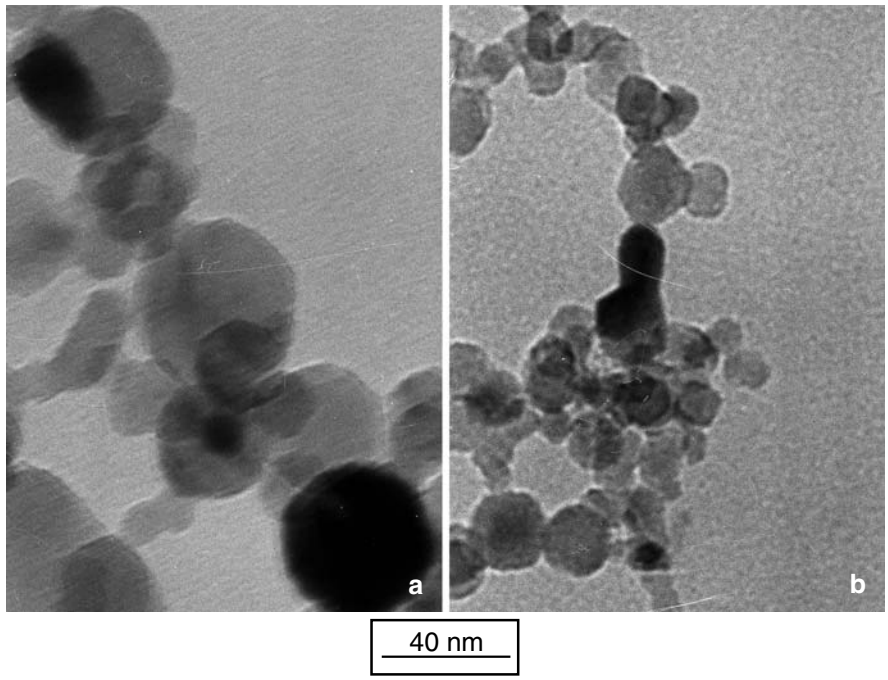

Fig. 26 Titania particles ex $TiCl_4$ produced in a premixed methane–oxygen flame. (Pratsinis 2006, private communication). (**a**) Reference material produced without electric field. (**b**) Product obtained with transversal electrical field of 1.6 kV cm^{-1}. The reduced particle size is well visible. Additionally, the size distribution of this product is significantly narrower

characteristics of the products and their industrial maturity are wide spread. Lastly, plasma processes may be classified into three groups:

- Processes working under ambient pressure. With respect to industrial application, these processes show the highest degree of maturity. The products obtained show typically a broad particle size distribution. Additionally, in most cases, significant agglomeration is observed. Generally, these processes operate at high temperatures.
- Processes operating at reduced pressure and comparably low temperatures. Selecting proper conditions for synthesis, the products obtained by these processes show a narrow size distribution. Additionally, it must be mentioned that these processes allow the synthesis of the smallest particles; particle sizes of 2 or 3 nm are achievable. The most successful variants apply microwaves as power source. Microwave processes working under reduced pressure are the only ones enabling the synthesis of coated particles.
- Some very special processes are in the early stages of development. In this group, flame processes combined with transversal electrical fields are most promising ones, as they deliver products with narrow particle size distribution. Flame processes have the well proven potential for the production of large quantities; therefore, one has to attribute a high potential of development for this combined process. As far as it is now visible, laser processes did not obtain importance, neither in science nor in industry.

Finally, it is necessary to mention the fact that, at least in the range of low power up to 5 kW, the power supply and the technical set-up of microwave systems are significantly cheaper as compared to devices using RF. Taking the better defined products into account, microwave plasma synthesis is the best choice for small scale production. As far as a comparison is possible at all, small microwave systems are cheaper than those working with tubular furnaces.

References

Anderson H, Kodas T, Smith DT (1989) Vapor phase processing of powders: plasma synthesis and aerosol decomposition. Ceram Bull 68:996–1000

Boulos MI (1984) Modelling of plasma processes. In: Szekely J, Apelian D (eds) Plasma processing and synthesis of materials symposium. North-Holland, New York, NY, USA, pp 53–60

Brenner JR, Harkness JBL, Knickelbein MB, Krumdick GK, Marshall CL (1997) Microwave plasma synthesis of

carbon-supported ultrafine metal particles. Nanostruct Mater 8:1–17

Buss RJ (1997) Rf-plasma synthesis of nanosize silicon carbide and nitride, SAND97–0039

Castillo IA, Munz RJ (2005) Inductively coupled plasma synthesis of CeO_2-based powders from liquid solutions for SOFC electrolytes. Plasma Chem Plasma Process 25: 87–107

Chau JLH, Hsu MK, Hsie CC, Kao CC (2005) Microwave plasma synthesis of silver nanopowders. Mater Lett 59:905–908

Chau CLH, Hsu MK, Kao CC (2006) Microwave plasma synthesis of Co and SiC-coated Co nanopowders. Mater Lett 60:947–951

Cota-Sanchez G, Soucy G, Huczko A, Lange H (2005) Induction plasma synthesis of fullerenes and nanotubes using carbon black-nickel particles. Carbon 43:3153–3166

Cruden BA, Cassell AM, Ye Q, Meyyappan M (2003) Reactor design considerations in the hot filament/direct current plasma synthesis of carbon nanofibers. J Appl Phys 94:4070–4078

David B, Pizúrová N, Schneeweiss O, Bezdicka P, Morjan I, Alexandrescu R (2004) Preparation of iron/graphite core-shell structured nanoparticles. J Alloy Compd 378: 112–116

Feldman Y, Frey GL, Homyonfer M, Lyakhovitskaya V, Margulis M, Cohen H, Hodes G, Hutchison JL, Tenne R (1996) Bulk synthesis of inorganic fullerene-like MS_2 from the respective trioxides and the reaction mechanism. J Am Chem Soc 118:5362–5367

Goortani BM, Mendoza N, Proulx N (2006) Synthesis of SiO_2 nanoparticles in RF plasma reactors: effect of feed rate and quench gas injection. Int J Chem React Eng 4: Article A33

Grabis J, Kuzjukevics A, Rasmane D, Mogensen M, Linderoth SJ (1998) Preparation of nanocrystalline YSZ powders by the plasma technique. J Mater Sci 33:723–728

He Y, Li X, Swihart MT (2005) Laser-driven aerosol synthesis of nickel nanoparticles. Chem Mater 17:1017–1026

Heberlein JVR (1989) Plasma technology in materials processing. Cryst Prop Prep 22–25:707–726

Kalyanaraman R, Yoo S, Krupshankara MS, Sudarshan TS, Dowding RJ (1998) Synthesis and consolidation of iron nanopowders. Nanostruct Mater 10:1379–1392

Kammler HK, Mädler L, Pratsinis SE (2001) Flame synthesis of nanoparticles. Chem Eng Technol 24:583–596

Kammler H (2002) Synthesis of oxide nanoparticles with closely controlled characteristics. PhD thesis, ETH Zürich #14622

Kaneko T, Odaka Y, Tada E, Hatakeyama R (2002) Generation and control of field-aligned flow velocity shear in a fully ionized collisionless plasma. Rev Sci Instrum 73: 4218–4222

Karthikeyan J, Berndt CC, Tikkanen J, Reddy S, Herman H (1997) Plasma spray synthesis of nanomaterial powders and deposits. Mater Sci Eng A238:275–286

Kim K (2005) Plasma synthesis and characterization of nanocrystalline aluminum nitride particles by aluminum plasma jet discharge. J Cryst Growth 283:540–546

Ko TS, Yang S, Hsu HC, Chu CP, Lin HF, Liao SC, Lu TC, Kuo HC, Hsieh WF, Wang SC (2006) ZnO nanopowders fabricated by dc thermal plasma synthesis. Mater Sci Eng B 134:54–58

Kortshagen U, Bhandarkar U (1999) Modeling of particulate coagulation in low pressure plasmas. Phys Rev E 60: 887–898

Langmuir I (1928) Oscillations in ionized gases. Proc Natl Acad Sci USA 14:627–637

Li Q, Sasaki T, Koshizaki N (1999) Pressure dependence of the morphology and size of cobalt (II, III) oxide nanoparticles prepared by pulsed-laser ablation. Appl Phys A69: 115–118

MacDonald AD (1966) Microwave breakdown in gases. Wiley & Sons, New York

Mangolini L, Jurbergs D, Rogojina E, Kortshagen U (2006) Plasma synthesis and liquid-phase surface passivation of brightly luminescent Si nanocrystals. Phys Stat Sol (c) 3:3975–3978

Manolache S, Denes F (2000) Synthesis of nanoparticles under cold-plasma conditions. J Photopolym Sci Technol 13: 51–62

Marzik JV, Suplinskas RJ, Wilke RHT, Canfield PC, Finnemore DK, Rindfleisch M, Margolies J, Hannahs ST (2005) Plasma synthesized doped B powders for MgB_2 superconductors. Physica C 423:83–88

Matsui I (2006) Preparation of magnetic nanoparticles by pulsed plasma chemical vapor synthesis. J Nanopart Res 8:429–443

Mohai J, Szepvölgyi I, Bertot M, Mohai J, Gubicza T, Ungar T (2001) Thermal plasma synthesis of zinc ferrite nanopowders. Solid State Ion 141–142:163–168

Morjan I, Alexandrescu R, Soare I, Dumitrache F, Sandu I, Voicu I, Crunteanu A, Vasile E, Ciupina V, Martelli S (2003) Nanoscale powders of different iron oxide phases prepared by continuous laser irradiation of iron pentacarbonyl-containing gas precursors. Mater Sci Eng C 23:211–216

Pratsinis SE (1998) Flame aerosol synthesis of ceramic powders. Prog Energy Combust Sci 24:197–219

Puretzky AA, Geohegan DB, Fan X, Pennycook SJ (2000) Dynamics of single-wall carbon nanotube synthesis by laser vaporization. Appl Phys A70:153–160

Rao NP, Girshick SL, McMurrey PH, Heberlein JVR (1999) US-patent #5,874,134

Schulz O, Hausner H (1987) Plasmasynthese keramischer Sinterpulver für Hochleistungskeramik. Elektrowärme, Int Edt 45:174–182

Schulz O, Hausner H (1992) Plasma synthesis of silicon nitride powders. Ceram Int 18:177–183

Schweigert IV, Schweigert J (1996) Coagulation in a low-temperature plasma. J Phys D 29:655–659

Shimada M, Azuma Y, Okuyama Y, Hayashi Y, Tanabe E (2006) Plasma synthesis of light emitting gallium nitride nanoparticles using a novel microwave-resonant cavity. Jpn J Appl Phys 45:328–332

Son S, Swaminathan R, McHenry MEJ (2003) Structure and magnetic properties of RF thermal plasma synthesized Mn and Mn–Zn ferrite nanoparticles. Appl Phys 93:7495–7497

Szekely J (1984) An overview of plasma processing. In: Szekely J, Apelian D (eds) Plasma processing and synthesis of materials symposium. North-Holland, New York, NY, USA, pp 1–11

Szépvölgyi J, Mohail I, Gubicza J, Sáray I (2004) RF plasma synthesis of ferrite nanopowders from metallurgical wastes. Key Eng Mater 264–268:2359–2362

Taylor PR, Vidal EE (1999) Thermal plasma synthesis of ceramic powders. In: Marquis EDS (ed) Powder materials: current research and industrial practices. Proceedings of symposium held during 1999 TMS fall meeting. TMS Miner Metals & Mater Soc, Warrendale, PA, USA, pp 173–185

Tekna Plasma Systems Inc (2007) Canada. http://www.tekna.com.

Tong L, Reddy RG (2005) Synthesis of titanium carbide nano-powders by thermal plasma. Scripta Materialia 52:1253–1258

Troitskiy VN, Domashnev IA, Kurkin EN, Grebtsova OM, Berestenko VI, Balikhin IL, Gurov SV (2003) Synthesis and characteristics of ultra-fine superconducting powders in the Nb–N, Nb–N–C, Nb–Ti–N–C systems. J Nanopart Res 5:521–528

Vissokov G, Grancharov I, Tsvetanov T (2003) On the plasma-chemical synthesis of nanopowders. Plasma Sci Technol 5(6):2039–2050

Vollath D (2007) Plasma synthesis of nanoparticles. Kona 25:39–55

Vollath D, Sickafus KE (1992a) Synthesis of nanosized ceramic powders by microwave plasma reactions. Nanostruct Mater 1:427–437

Vollath D, Sickafus KE (1993) Synthesis of nanosized ceramic nitride powders by micro-wave supported plasma reactions. Nanostruct Mater 2:451–456

Vollath D, Szabó DV (1994) Nanocoated particles: a special type of ceramic powder. Nanostruct Mater 8:927–938

Vollath D, Szabó DV (1998) Synthesis of nanocrystalline MoS_2 and WS_2 in microwave plasma. Mater Lett 35: 236–244

Vollath D, Szabó VS (2000) Nanoparticles from compounds with layered structures. Acta Materialia 48:953–967

Vollath D, Szabó DV (2002) Synthesis of nanopowders by the microwave plasma process—basic considerations and perspectives for scaling-up. In: Choy KL (ed) Innovative processing of films and nanocrystalline powders. Imperial College Press, London

Vollath D, Szabó DV (2004) Synthesis and properties of nanocomposites. Adv Eng Mater 6:117–127

Vollath D, Szabó DV (2006) The microwave plasma process—a versatile process to synthesise nanoparticulate materials. J Nanopart Res 8:417–418

Vollath D, Szabó DV, Fuchs J (1999) Synthesis and properties of ceramic-polymer composites. Nanostruct Mater 12:433–438

Wang Y, Qin Y, Li G, Cui Z, Zhang Z (2005) One-step synthesis and optical properties of blue titanium suboxide nanoparticles. J Cryst Growth 282:402–406

Wang Z, Liu Y, Zeng X (2006) One-step synthesis of γ-Fe_2O_3 nanoparticles by laser ablation. Powder Technol 161: 65–68

Zak A, Feldman Y, Alperovich V, Rosentsveig R, Tenne R (2000) Growth mechanism of MoS_2 fullerene-like nanoparticles by gas-phase synthesis. J Am Chem Soc 122:11108–11116

Ziemann PJ, Kittelson DB, McMurry PH (1996) Effects of particle shape and chemical composition on the electron impact charging properties of submicron inorganic particles. J Aerosol Sci 27:587–606